Available online at
https://mijuitm.com.my

e-ISSN: 2735-0703

Mathematical Sciences and Informatics Journal 6(1) 2025, 38 – 52.

Mathematical Sciences and Informatics Journal

A Data-Driven SIR Model Analysis of COVID-19 Interventions in Malaysia

Abdul Basit[1*], Jasni Mohamad Zain[2], Hafiza Zoya Mojahid[1], Abdul Kadir Jumaat[2], Nur'Izzati Hamdan[1]

[1]*College of Computing, Informatics and Mathematics, Universiti Teknologi Mara, Shah Alam, Selangor, Malaysia*
[2]*Institute of Big Data Analytics and Artificial Intelligence (IBDAAI), Universiti Teknologi Mara, Shah Alam, Selangor, Malaysia*

ARTICLE INFO

Article history:
Received 14 March 2025
Revised 28 March 2025
Accepted 11 April 2025
Online first
Published 30 April 2025

Keywords:
Mathematical Model
SIR
Parameters
COVID-19
Forecasting
Infection

DOI:
10.24191/mij.v6i1.4625

ABSTRACT

COVID-19 emerged in late 2019 and rapidly spread worldwide, posing a significant challenge to effective outbreak management. This study employs the Susceptible-Infected-Recovered (SIR) model to understand the transmission dynamics of COVID-19 in Malaysia, with a population of 34.3 million. Focusing on key phases implemented like the Movement Control Order (MCO) and Recovery Movement Control Order (RMCO), the research evaluates infection rates, recovery dynamics, and reproduction numbers using real-world data from the Johns Hopkins University COVID-19 Dashboard. During the MCO phase (18 March 2020 to 3 May 2020), the transmission rate was 0.0806, the recovery rate was 0.0309, and the basic reproduction number (R_0) was 2.607, with 90.52% of the population remaining susceptible post-phase. The RMCO phase (10 June 2020 to 31 March 2021) saw reduced transmission and recovery rates of 0.0880 and 0.0518, respectively, resulting in an R_0 of 1.698 and 68.97% of the population remaining susceptible. The peak infection rate during RMCO was significantly lower (1.698%), with the infection peak forecasted for 11 December 2020. The findings offer actionable insights for policymakers, demonstrating how targeted lockdown measures can significantly reduce transmission rates and delay infection peaks while emphasizing the SIR model's utility in providing timely insights during evolving public health crises.

1. INTRODUCTION

Infectious diseases caused by various pathogens pose significant risks to public health and societal stability. These diseases can spread among individuals, animals, and even across species, creating a complex

[1*] Corresponding author. *E-mail address*: 2021691374@student.uitm.edu.my
https://doi.org/10.24191/mij.v6i1.4625

transmission network (Ahn et al., 2020). Meanwhile, a subset of these pathogens includes parasites, the majority of which are bacterial in nature. Disorders caused by parasites are classified as parasitic diseases. Monitoring and mitigating the spread of infectious diseases require proactive measures from epidemic prevention divisions. These agencies must remain vigilant, promptly reporting outbreaks to relevant authorities to safeguard public health (Hanson et al., 2020). Transmission of infectious diseases can occur through diverse pathways, including air, water, and contaminated food sources. The impacts of such outbreaks are far-reaching, affecting both the economic and physical well-being of affected populations. This is particularly evident in the absence of vaccines, as was the case during the early stages of the COVID-19 pandemic. Without immediate vaccine availability, prediction and prevention became critical strategies for controlling the virus's spread (Nicolle et al., 2019).

Established on datasets from the World Health Organization (WHO), the global death toll attributed to COVID-19 has surpassed 5 million individuals. Early public health interventions significantly mitigated the development of the virus and reduced mortality. COVID-19 primarily spreads through respiratory droplets and direct human contact. The virus has an incubation period of 1 to 14 days, contrasting with the longer incubation periods of 14 to 28 days seen in many transmissible illnesses. Notably, COVID-19 is infectious during incubation, facilitating rapid person-to-person transmission (Basit et al., 2024). The clinical manifestations of COVID-19 include fever, dry cough, and fatigue, with some individuals experiencing sore throats, nasal congestion, and diarrhea. Severe cases often lead to breathing difficulties and low blood oxygen levels approximately seven days after infection onset (Brosnahan et al., 2020). These characteristics underscore the need for rapid detection and intervention to curb transmission and reduce severe outcomes.

(i) Region-Specific Analysis: Unlike global models, this study focuses specifically on Malaysia, incorporating real-time intervention phases (MCO and RMCO) to assess their impact on COVID-19 transmission.

(ii) Time-Varying Reproduction Number Estimation: By leveraging empirical data, the study evaluates changes in the reproduction number (R_0) over time, reflecting dynamic transmission patterns.

(iii) Effective Approach: The study employs the classical SIR model rather than complex modifications, ensuring computational efficiency while maintaining accurate disease progression assessments.

By addressing these aspects, this research enhances the understanding of COVID-19 transmission dynamics in Malaysia and provides a foundation for future epidemic modeling in similar regional contexts.

2. LITERATURE REVIEW

This section reviews various studies that have employed the SIR framework and its modifications to evaluate transmission and project COVID-19 patterns. In a study conducted by the researchers introduced a modified SIR model, incorporating factors such as herd immunity, behavioral transmission rates, and the effects of lockdowns, finding that prolonged lockdowns could reduce mortality by one-third; however, the model's complexity increases computational demands, making it less practical for real-time forecasting (Mojahid et al., 2024; Bayraktar et al., 2020). Also, another type of research proposed the Susceptible-Infected-Machine-Learning-Recovered (SIMLR) model, integrating machine learning to forecast new infections up to four weeks ahead, enhancing accuracy with data-driven insights. Still, the model's reliance on vast amounts of data introduces uncertainty in its forecasting (Vega et al., 2022). A study applied the SIR model to evaluate epidemic risks across various countries, offering a simple yet effective method for assessing the consequences of prematurely lifting quarantine measures. However, its assumptions of constant parameters may not fully capture dynamic changes in transmission over time (Nesteruk, 2020).

https://doi.org/10.24191/mij.v6i1.4625

Another Research presents a time-dependent SIR approach that monitors transmission and recovery rates over time while examining the effect of undetectable infections on disease spread; however, the model's reliance on time-varying parameters increases its complexity, potentially leading to computational inefficiencies (Chen et al., 2020). Another study introduced a fractional-order discrete SIR model capable of adapting to periodic fluctuations in infection numbers. However, the model's assumptions regarding periodicity may not fully capture abrupt changes in disease dynamics (Djenina et al., 2022). Additionally, a study presented a multi-level SIR model designed to identify and model disease waves in real-time. Still, its computational demands may hinder its application in large-scale or real-time forecasting (Perakis et al., 2023). A study created a prognostic SIR model for the COVID-19 pandemic in Colombia, adjusting the basic reproduction number (R_0) to explore various scenarios; however, the model's reliance on country-specific data may limit its generalizability to other regions (Lounis & Bagal, 2020).

A team of scholars introduced a Susceptible-Contacts-Exposed-Infected-Recovered (SCEIR) model that includes factors like close contacts and self-protection, offering insights for epidemic prevention strategies, but the complexity of the model may make it difficult to implement in resource-limited settings (Ni et al., 2022). Another research employed the SIR model to estimate coefficients and forecast the potential end time and turning point of COVID-19 in the United States. However, uncertainties in initial assumptions and parameter estimation may reduce the accuracy of the long-term forecast (Amiri Mehra et al., 2020). Research used an implicit time-discrete SIR model to forecast COVID-19 trends in Fiji, achieving strong alignment with reported data; however, the model's discrete nature may limit its ability to capture continuous changes in disease dynamics (Singh et al., 2022).

A study applied the SIR model to track COVID-19 spread in Italy, India, South Korea, and Iran, forecasting trends from March to September 2020. While the model detected early infection spikes and second waves, its reliance on published data limited its ability to fully assess government interventions (Cooper et al., 2020). Another study utilized the SIR model to analyze COVID-19 transmission dynamics, relying on real-world data and predefined compartment conditions. However, its assumptions of a well-mixed population and constant transmission rates limit its ability to capture real-world complexities such as demographic and geographic variability (Wu, 2023). A group of researchers applied the SIR model to analyze COVID-19 spread in four regions of India, simulating the impact of a two-month nationwide lockdown on the contact rate. While the model provided insights into transmission dynamics, its reliance on short-term data and assumptions of a homogeneous population may limit its accuracy in capturing long-term pandemic trends (Saxena et al., 2021).

Furthermore, research simulated the COVID-19 epidemic in Nigeria using the SIR model, optimizing parameters with Maximum Likelihood Estimation and the Nelder-Mead algorithm. However, the predicted peak did not align with actual trends, likely due to unaccounted external factors influencing transmission dynamics (Duan, 2021). Another study opted the SIR model to forecast the COVID-19 epidemic in Malaysia, utilizing its compartmental structure to model disease spread. However, the model's assumptions of a closed population and constant transmission rates may limit its accuracy in capturing real-world variations in mobility, interventions, and reinfection risks (Zenian, 2022). Additionally, a study modified SIR model to forecast the COVID-19 epidemic in India, incorporating factors like flattening the curve, herd immunity, and dynamic population changes. However, potential limitations in model assumptions and unaccounted transmission variables may affect the accuracy of its projections (Venkatasen et al., 2020).

Building upon these studies, this research employs the SIR model to analyze COVID-19 transmission dynamics in Malaysia. This study evaluates changes in infection rates, recovery patterns, and reproduction numbers by analyzing real-world COVID-19 data from the Johns Hopkins University COVID-19 Dashboard (CSSE, 2024). The dataset includes reported cases, recoveries, and fatalities recorded in Malaysia. Additionally, key intervention phases, such as the Movement Control Order (MCO) and the Recovery Movement Control Order (RMCO), were examined to assess their impact on transmission dynamics. The data were systematically collected, ensuring consistency in tracking the progression of the

https://doi.org/10.24191/mij.v6i1.4625

outbreak across different time periods. Unlike models that incorporate additional complex parameters, this study maintains the classical SIR structure while leveraging empirical data to assess the effectiveness of government-imposed measures in mitigating the epidemic's spread. The findings provide valuable insights into how targeted interventions impact disease progression and inform future public health strategies. To achieve these objectives, the following section outlines the methodology employed in this study, detailing the dataset acquisition, parameter estimation, and evaluation techniques used to assess the spread of COVID-19 in Malaysia.

3. METHODOLOGY

3.1 SIR Model

The SIR mathematical model, a powerful mathematical model for depicting infectious diseases, was developed by Kermack and McKendrick in 1927 (Moein et al., 2021). This section outlines the standard framework of the SIR model used to illustrate COVID-19 spread in Malaysia. Fig. 1 provides a schematic of the SIR model, which is employed to describe the dynamics of infectious disease transmission. The model consists of three compartments (Putra et al., 2019); (Mbuvha & Marwala, 2020).

Fig. 1. The schematic diagram of the SIR Model.

(i) Susceptible (S): Find the differences between before and after.

(ii) Infected (I): Populations who currently have the infection and are capable of spreading it to others.

(iii) Recovered (R): Populations who have previously been infected with the disease and have since recovered. They are no longer capable of transmitting the infection, but they have permanent immunity.

The arrows in Figure 1 illustrate the flow of population between compartments. The evolution rate from the vulnerable to the diseased compartment is governed by the disease transmission rate. In contrast, the movement from the diseased to the recovered group is controlled by the recovery rate. The SIR model is a simple yet effective tool for analyzing infectious disease dynamics, including COVID-19. The equations for the SIR model based on ordinary differential equations (1-3) are stated as (Rahimi et al., 2021).

$$\frac{dS}{dt} = -\beta IS. \tag{1}$$

$$\frac{dI}{dt} = \beta IS - \gamma I. \tag{2}$$

$$\frac{dR}{dt} = \gamma I. \tag{3}$$

The SIR model was chosen for its simplicity, practicality, and effectiveness in capturing disease spread dynamics in the early outbreak stages. The SIR model provides a simple yet reliable approach for analyzing and predicting pandemic trends, especially when data is limited. The model assumes a well-mixed population (Homogeneity) where each individual has an equal probability of interacting with others,

https://doi.org/10.24191/mij.v6i1.4625

characterized by two key parameters: β (transmission rate) and γ (recovery rate) (Yunus et al., 2021). These parameters provide a fundamental understanding of the interplay between disease transmission and recovery. The core premise of the SIR model is that infected individuals interact with others, but infection can only spread to those who are susceptible. The likelihood of encountering a susceptible individual is proportional to their share of the total population, denoted as N=S+I+R, where N remains constant over time, implying no births, deaths, or migration, which simplifies computations. However, the model assumes no reinfection after recovery, which is a limitation when considering diseases with waning immunity or variants that may cause reinfection. Recognizing this limitation, ongoing research aims to extend the model to account for infections with loss of immunity. Despite this constraint, the SIR model's balance of simplicity and explanatory power makes it an invaluable approach for understanding and managing infectious disease dynamics, particularly in the context of emerging pandemics like COVID-19. According to United Nations (UN) data, the estimated population of Malaysia in mid-2023 was 34,308,525 people (Worldometer, 2024). The parameters of the mathematical model considered as Table 1 presents.

Table 1. Parameters of SIR Model.

Parameter	Detail
β (Beta)	The rate at which the disease is transmitted.
γ (Gamma)	The rate at which the population recover from the infection.
R_0 (Basic Reproduction)	The number of individuals who are infected by a single contagion case in a group where everyone is vulnerable.

Therefore, the ratio of population magnitude (N) was approximated as 34,345,167 for the SIR modeling of Malaysia. When infection is absent or when I + R = 0, the substitution of $S \approx N$ into equation (2) leads to the derivation of the subsequent equation (4).

$$\frac{dI}{dt} \sim I(\beta - \gamma). \tag{4}$$

Subsequently, through the process of integrating equation (4), we acquired the ensuing equation (5).

$$I = I_o e^{(\beta-\gamma)t}. \tag{5}$$

3.2 Derivation of β and m Values

During the initial outbreak of the infection, a significant portion of the population is vulnerable, namely $S \approx N$. As a result, the initial increase of Infection(t) takes place in an exponential manner, as shown in equation (6).

$$\frac{dI}{dt} \sim mI. \tag{6}$$

Here, the constant term $m = \beta$ - γ symbolizes the variance between the transmission and recovery rates, and we get equation (7).

$$I(\,t\,) \sim I_0 e^{mt}. \tag{7}$$

The value of m can be approximated through log-plot data analysis, employing the least squares method and regression to achieve the optimal linear fit, equation (8).

https://doi.org/10.24191/mij.v6i1.4625

$$\ln I = mt + \ln I_0. \tag{8}$$

3.3 Derivation of γ Values

Assume I(t) = I0 (constant). Then, we derive the succeeding equation (9).

$$\frac{dR}{dt} = \gamma I_o. \tag{9}$$

Further, by incorporating equation (9), we derived the succeeding equation (10).

$$R(t) = \gamma t I_o. \tag{10}$$

If suppose it takes t = T days to recover, then γ = 1/T. Therefore, we acquired the subsequent equation (11).

$$\gamma \approx 1/T. \tag{11}$$

Here, T is the recovery epoch. By equation (3), for an alteration in the period of dt = a, it acquired the subsequent calculation as equation (12).

$$\frac{R(t+a)}{a} = \gamma I. \tag{12}$$

3.4 Derivation of Basic Reproduction Number (R_0)

The basic reproduction number represents the proportion of the transmission rate to the recovery rate. This number is significant because it indicates how contagious an infectious disease is; an R_0 larger than 1 means the infection will probably expand through the inhabitants, while an R_0 lower than 1 suggests the infection will ultimately die out. It can be mathematically termed as equation (13).

$$R_0 = \frac{\beta}{\gamma}. \tag{13}$$

It characterizes the average sum of individuals that one diseased individual will pass the disease to. Based on R_0, the following equations (14) and (15) can be derived.

$$1 - \frac{1}{R_0}\left(1 - ln\frac{1}{R_0}\right) = i_{\max}\ , \tag{14}$$

and,

$$1 - \frac{1}{R_0}\left(1 - ln\frac{1}{R_0}\right) = i_{\max}\ . \tag{15}$$

The R_0 can be reduced if strict procedures of control and measures are implemented. Hence, we achieved the calculated parameters of the SIR model by the least square method and regression best line of fit. In this study, the dataset was obtained from the 2019 Novel Coronavirus Visual Dashboard, curated by the Johns Hopkins University Center for Systems Science and Engineering (JHU-CSSE). The SIR model, implemented in Python language and customized to analyze Malaysia's dataset, was executed on the Google Colab platform, leveraging its computational capabilities for efficient processing. Additionally, future dates for key milestones were calculated using an online date calculator to ensure precise temporal predictions and facilitate the interpretation of the model's outcomes (BizCalcs, 2024).

https://doi.org/10.24191/mij.v6i1.4625

3.5 Derivation of Peak of Infection

Determining the maximum infection rate and identifying the remaining susceptible population after the peak of infection is crucial for understanding the trajectory of an epidemic. By pinpointing the infection peak rate, we can gauge the most critical phase of the outbreak, which is essential for resource allocation and healthcare preparedness. Additionally, assessing the number of individuals still susceptible post-peak provides insights into potential risks for subsequent waves and helps in planning long-term public health strategies. These determinations enable a comprehensive evaluation of the epidemic's impact and the effectiveness of interventions implemented by evaluating equation (1) by equation (2), the achieved equation (16).

$$\frac{dI}{dS} = \frac{\gamma}{\beta} N \frac{1}{S} - 1. \tag{16}$$

By integrating both sides, the following equation (17) was obtained.

$$-S + \frac{\gamma}{\beta} N log S + C = I, C \text{ is constant}. \tag{17}$$

At the beginning of infection, the ratio of infection in equation (17) is critically low, Hence, S≈N (equal total size of population). Therefore, S~N, I~0 and t=0. Hence, by integrating these ratios into equation (17), the derived equation (18).

$$N\left(1 - \frac{\gamma}{\beta} lnN\right) = C. \tag{18}$$

By substituting the value of C from equation (18) into equation (17), we obtained the following equation (19).

$$N - S + \frac{\gamma}{\beta} N ln \frac{S}{N} = I. \tag{19}$$

Equation (19) holds for all time points throughout the outbreak. Initially, the number of infected individuals (I) follows an exponential growth pattern, reaches a maximum, and then gradually declines toward zero. To analyze the dynamics, it is essential to determine the proportion of the infected population at the peak (I_{max}) and the fraction of the population that remains susceptible and has not yet contracted the disease. Equations (2) and (19) represent the differential equation describing the infection rate and its corresponding solution, respectively. To, we must undertake $S=N_s$, $I=N_i$, and $R=N_r$. Then, s, r and I denote the ratio of total infected, susceptible and recovered cases. Hence, the achieved equations (20) and (21).

$$\frac{di}{dt} = i(\beta s - \gamma), \tag{20}$$

and,

$$1 - s + \frac{\gamma}{\beta} ln s = i. \tag{21}$$

At the peak infection, di/dt=0, susceptible cases are achieved by the equation (22).

$$s = \frac{\beta}{\gamma}. \tag{22}$$

https://doi.org/10.24191/mij.v6i1.4625

By integrating equation (22) into equation (21), the achieved equation (23).

$$1+\frac{\gamma}{\beta}\left(ln\frac{\gamma}{\beta}-1\right)=i_{max}. \tag{23}$$

The fraction of infected individuals at the highest significantly decreased during each lockdown period in Malaysia. Now, we need to determine $S_{inf}=\lim_{t\to\infty}S(t)$, which represents the percentage of people who remain susceptible after the infection has subsided. It's important to note that i=0 as t approaches infinity at the conclusion of the infection. Consequently, equation (21) can be reformulated as equation (24).

$$1-s+\frac{\gamma}{\beta}lns=0. \tag{24}$$

Equation (21) can be resolved statistically to determine the rate of ‘s’. Using the dataset from Malaysia, we calculated the values of S_{inf}, representing the remaining susceptible cases. These calculations provide valuable insights into the peak infection rate and the remaining susceptible population after the epidemic has subsided. By determining the peak infection, public health officials can better allocate resources and prepare for future waves of the disease. Additionally, understanding the proportion of susceptible individuals S_{inf} at the conclusion of the outbreak is critical for planning long-term strategies aimed at mitigating future transmission and enhancing vaccination campaigns. The application of this model to Malaysia's COVID-19 data offers essential guidance in evaluating the effectiveness of public health interventions and predicting potential future risks.

4. RESULTS AND DISCUSSION

4.1 Derivation of Peak of Infection

Table 2 presents the experimental results of the spread of infection, recovery and basic reproduction number during the Movement Control Order (MCO) period.

Table 2. Calculated Parameters of SIR model by Least Square Method for MCO.

Phase	Start Date	End Date	Average (β)	Average (γ)	Average (R_0)	Value of m (β-γ)
MCO Phase	18-Mar-20	3-May-20	0.0806	0.0309	2.607	0.0497

During the MCO phase in Malaysia, implemented from 18 March 2020 to 3 May 2020, the infection dynamics were significantly influenced by stringent public health measures aimed at limiting the spread of COVID-19. The calculated parameters of the SIR model during this period reveal an average transmission rate (β) of 0.0806 and a recovery rate (γ) of 0.0309, resulting in a basic reproduction number (R_0) of 2.607. This indicates that, on average, one infected individual had the potential to infect approximately 2.6 others during the early MCO phase. However, the enforcement of social distancing measures, travel restrictions, and public awareness campaigns likely contributed to the gradual reduction of infection and the difference between the rate of infection and recovery rate, denoted as m (0.0497), as shown in Fig. 2.

https://doi.org/10.24191/mij.v6i1.4625

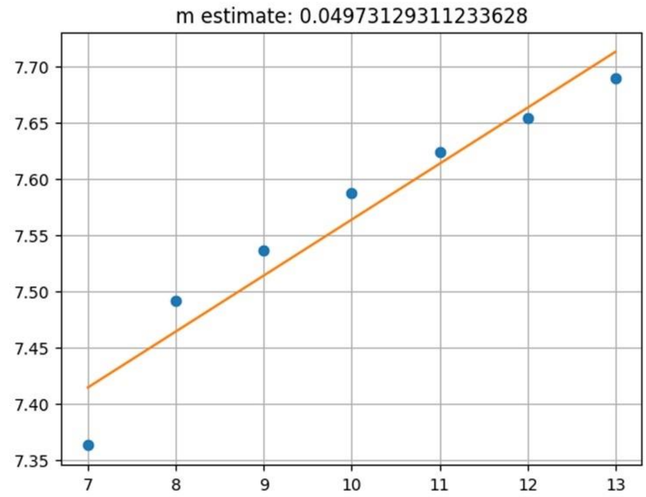

Fig. 2. Estimated SIR model parameters during the MCO phase

It was observed that 90.52% of the population remained susceptible to COVID-19 by the end of this period, as shown in Table 3.

Table 3. Remaining Susceptible Population During the MCO Phase.

Phase	Start Date	End Date	S_{inf} (%)
MCO Phase	18-Mar-20	3-May-20	90.52

Malaysia's total population of 34,345,167 translates to approximately 31,092,820 individuals who have not yet contracted the virus. The high percentage of remaining susceptible individuals underscores the effectiveness of the MCO in curbing the spread of infections during its enforcement. By limiting mobility, enforcing social distancing, and promoting public health measures, the MCO successfully reduced exposure to the virus and prevented a large-scale outbreak. However, the significant proportion of susceptible individuals also highlighted the continued risk of future waves of infection if restrictions were lifted prematurely or if vaccination campaigns were delayed. This emphasizes the importance of sustained public health strategies to protect the uninfected population and achieve broader immunity. The data presented in Table 4 provides insights into the estimated peak infection dynamics during the MCO phase.

Table 4. Estimated Peak Infection Metrics During the MCO Phase.

Phase	Start Date	End Date	I_{max} (%)	Estimated Infection peak
MCO Phase	18-Mar-20	3-May-20	24.9	9-Oct-20

An infection peak (I_{max}) value of 24.9% suggests that nearly one-quarter of the population would be actively infected at the peak under the continued MCO measures. The forecasted peak infection date of 9th October 2020 aligns with the model's projections, as shown in Fig. 3, emphasizing the critical period of the outbreak's progression. This estimation underscores the importance of sustained control measures in mitigating the spread of infection and preventing healthcare system overburdening. It highlights the necessity of ongoing public health interventions to manage and reduce the epidemic's severity.

https://doi.org/10.24191/mij.v6i1.4625

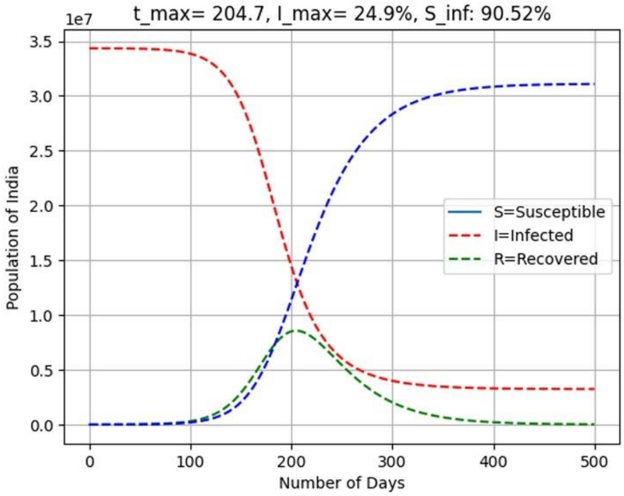

Fig. 3. SIR Model Simulation for the MCO Phase, showing the dynamics of Susceptible, Infected, and Recovered populations over time.

4.2 Recovery Movement Control Order

Table 5 presents the experimental results of the spread of infection, recovery and basic reproduction number during the Recovery Movement Control Order (RMCO) period.

Table 5. Calculated Parameters of SIR model by Least Square Method for RMCO.

Phase	Start Date	End Date	Average (β)	Average (γ)	Average (R_0)	Value of m (β-γ)
RMCO Phase	10-Jun-20	31-Mar-21	0.0880	0.0518	1.698	0.0361

During the RMCO phase, spanning from 10th June 2020 to 31st March 2021, the parameters of the SIR model provided significant insights into the dynamics of COVID-19 spread and recovery. The average transmission rate (β) was recorded at 0.0880, while the average recovery rate (γ) was 0.0518, resulting in a net growth rate ($m=\beta-\gamma$) of 0.0361. The basic reproduction number (R_0) during this phase dropped significantly to 1.698, compared to the 2.607 observed during the MCO phase. This decline reflects improved control of the infection spread due to effective public health interventions, including social distancing measures, partial reopening under strict guidelines, and public compliance with health advisories. The reduced R_0 indicates that, on average, each infected individual was transmitting the virus to fewer than two others, signifying a shift toward containment of the epidemic. Additionally, the smaller value of m suggests a closer balance between infection and recovery rates, further supporting the view that the RMCO measures successfully mitigated the pandemic's progression while allowing for some degree of normalcy to resume. These findings highlight the importance of adaptive, data-driven strategies in managing the spread of infectious diseases.

These results indicate a noticeable reduction in the net growth rate compared to earlier phases, reflecting the impact of eased restrictions coupled with sustained public health measures. The lower value of m suggests that while infections continued to occur, the balance between transmission and recovery leaned more favorably toward recovery during this phase. The RMCO measures allowed for a degree of economic and social activity to resume while maintaining sufficient control over the epidemic's trajectory, emphasizing the effectiveness of a phased and adaptive approach to pandemic management. Figure 4 highlights the calculated graph of the *m* value.

https://doi.org/10.24191/mij.v6i1.4625

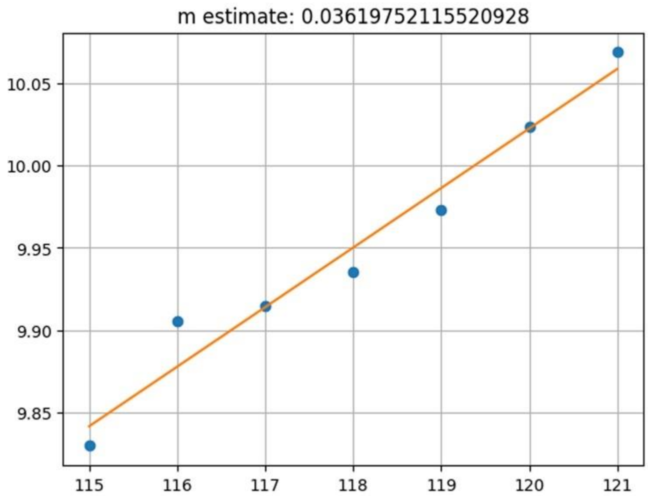

Fig. 4. Estimated SIR model parameters during the RMCO phase

It was observed that 68.97% of the population remained susceptible to COVID-19 by the end of this period, as shown in Table 6.

Table 6. Remaining Susceptible Population During the RMCO Phase.

Phase	Start Date	End Date	S_{inf} (%)
RMCO Phase	10-Jun-20	31-Mar-21	68.97

The percentage of the population that remained susceptible to infection S_{inf} dropped significantly to 68.97%. This indicates a substantial reduction in the susceptible population compared to the 90.52% recorded during the earlier MCO phase. The decline in the susceptible population during the RMCO phase highlights the ongoing transmission and progression of infections, albeit at a slower pace due to the partial reopening and improved public health measures. The reduction in susceptibility suggests that more individuals either recovered from infection or developed immunity during this period. The 31.03% of the population that had experienced an infection or gained immunity underscores the impact of the extended timeline and the modified control measures under RMCO. While the relaxed restrictions allowed for economic recovery and social activities, the data emphasizes the importance of continued vigilance to prevent further outbreaks. This insight provides a basis for understanding the effectiveness of RMCO in balancing infection control with societal and economic needs. The data presented in Table 7 provides insights into the estimated peak infection dynamics during the RMCO phase.

Table 7. Estimated Peak Infection Metrics During the RMCO Phase.

Phase	Start Date	End Date	I_{max} (%)	Estimated Infection peak
RMCO Phase	10-Jun-20	31-Mar-21	1.698	11-Dec-20

The estimated peak infection metrics reveal significant insights into the epidemic's progression under the modified control measures. The peak infection rate (I_{max}) during this phase was significantly lower, at 1.698%, compared to the 24.9% observed during the earlier MCO phase. The estimated peak of infection occurred on 11th December 2020, a few months after the phase began. This reduction in the peak infection

https://doi.org/10.24191/mij.v6i1.4625

rate reflects the effectiveness of RMCO policies in curbing the virus's spread while gradually resuming economic and social activities. The low Imax suggests that a combination of public health measures, including mask mandates, physical distancing, and targeted testing and tracing, helped to mitigate the outbreak's intensity during this phase. Furthermore, the delayed timing of the peak infection compared to the earlier phase highlights the extended timeline over which infections were controlled and managed. Figure 5 displays the SIR simulation during the RMCO phase.

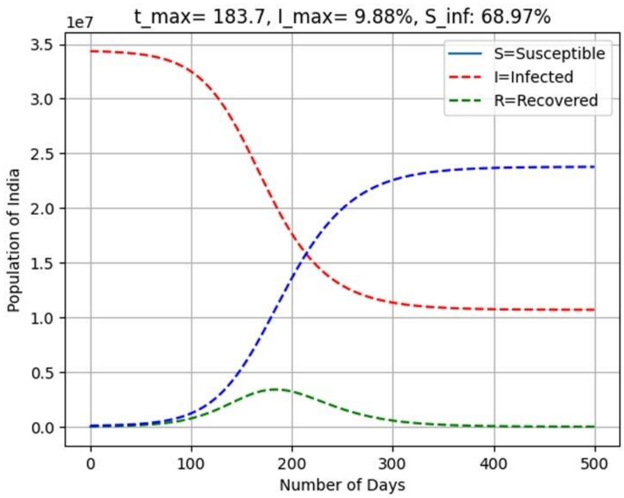

Fig. 5. SIR Model Simulation for the RMCO Phase, showing the dynamics of Susceptible, Infected, and Recovered populations over time.

The RMCO phase's metrics underscore the importance of adapting public health strategies to maintain a balance between reopening and managing infection risks. By achieving a lower infection peak and spreading the infections over a longer period, the healthcare system was better equipped to manage cases, ensuring resources were not overwhelmed while minimizing disruptions to daily life. An unexpected observation was the substantial proportion of the population that remained susceptible by the end of both phases as 90.52% in the MCO and 68.97% in the RMCO. While high susceptibility aligns with strict intervention success, it also indicates that herd immunity had not been achieved, leaving a large fraction of the population vulnerable to future outbreaks. Additionally, despite an increase in the average transmission rate (β) from 0.0806 in MCO to 0.0880 in RMCO, the net growth rate (m) dropped significantly due to a higher recovery rate (γ). This suggests that although infections continued, improved medical interventions, public awareness, and behavioral adaptations contributed to a more balanced epidemic trajectory.

5. CONCLUSION

This study provides a comprehensive analysis of COVID-19 transmission dynamics in Malaysia using the Susceptible-Infected-Recovered (SIR) model, offering critical insights into the efficacy of public health interventions during the early stages of the pandemic. By evaluating the Movement Control Order (MCO) and Recovery Movement Control Order (RMCO) phases, we observe significant variations in infection rates, recovery dynamics, and reproduction numbers. The results underscore the effectiveness of these interventions in curbing the spread of the virus, with a marked reduction in the basic reproduction number (R_0) during the RMCO phase compared to the MCO phase.

https://doi.org/10.24191/mij.v6i1.4625

Despite these efforts, the model highlights a substantial portion of the population remaining susceptible, indicating the ongoing risk of further outbreaks. The SIR model proved to be a valuable tool in understanding the epidemic's progression, offering an accessible yet powerful framework for decision-making in public health management, especially when limited data is available. However, underreporting of cases, particularly among asymptomatic or mildly symptomatic individuals, can lead to an underestimation of infection rates, affecting the accuracy of predictive models. Additionally, delays in data collection and reporting may introduce temporal distortions, making real-time model predictions less reliable. The findings underscore the importance of adaptive, phased intervention strategies in pandemic management. The substantial reduction in R_0 during RMCO highlights the potential of combining targeted public health measures with gradual reopening to balance economic and social activities while maintaining control over the epidemic.

Policymakers can use these insights to optimize future response strategies, ensuring that public health interventions remain flexible and responsive to real-time data. Moreover, the high percentage of susceptible individuals by the end of both phases suggests the need for complementary measures such as widespread vaccination and enhanced testing. Without these, lifting restrictions too soon could lead to resurgence, as seen in several regions that relaxed measures prematurely. This reinforces the importance of integrating forecasting models into decision-making frameworks to anticipate outbreak trends and allocate resources effectively.

6. ACKNOWLEDGEMENTS/FUNDING

The authors gratefully acknowledge the Universiti Teknologi MARA (UiTM), Shah Alam branch and Institute for Big Data Analytics and Artificial Intelligence (IBDAAI).

7. CONFLICT OF INTEREST STATEMENT

The authors agree that this research was conducted in the absence of any self-benefits, commercial or financial conflicts and declare the absence of conflicting interests with the funders.

8. AUTHORS' CONTRIBUTIONS

Abdul Basit carried out the research, wrote and revised the article. Prof.Dr.Jasni Mohamad Zain conceptualised the central research idea and provided the theoretical framework. Dr.Abdul Kadir Jumaat and Dr.Nur'Izzati Hamdan designed the research, supervised research progress; Hafiza Zoya Mojahid anchored the review, revisions and executed the article submission.

REFERENCES

Ahn, N. Y., Park, J. E., Lee, D. H., & Hong, P. C. (2020). Balancing personal privacy and public safety during COVID-19: The case of South Korea. *Ieee Access*, *8*, 171325-171333. https://doi.org/10.1109/access.2020.3025971

Amiri Mehra, A. H., Shafieirad, M., Abbasi, Z., & Zamani, I. (2020). Parameter Estimation and Prediction of COVID-19 Epidemic Turning Point and Ending Time of a Case Study on SIR/SQAIR Epidemic Models. *Computational and Mathematical Methods in Medicine*, *2020*(1), 1465923. https://doi.org/10.1155/2020/1465923

Basit, A., Mohamad Zain, J., Jumaat, A. K., Hamdan, N. I., & Mojahid, H. Z. (2024). Predicting COVID-19 trends: a deep dive into time-dependent SIRSD with deep learning technique. *Malaysian Journal of Computing (MJoC)*, *9*(2), 1955-1978. https://doi.org/10.24191/mjoc.v9i2.27425

Bayraktar, E., Cohen, A., & Nellis, A. (2021). A macroeconomic SIR model for COVID-19. *Mathematics*, *9*(16), 1901. https://doi.org/10.1101/2020.06.22.20137711

BizCalcs. (2024, July 15). Date calculator. http://date.bizcalcs.com/Calculator.asp?Calc=Find-Future-Date

Brosnahan, S. B., Jonkman, A. H., Kugler, M. C., Munger, J. S., & Kaufman, D. A. (2020). COVID-19 and respiratory system disorders: current knowledge, future clinical and translational research questions. *Arteriosclerosis, thrombosis, and vascular biology*, *40*(11), 2586-2597. https://doi.org/10.1161/atvbaha.120.314515

Center for Systems Science and Engineering (CSSE) at Johns Hopkins University. (2024, December 10). Time series data set for COVID-19 cases [Dataset]. *Kaggle*. https://www.kaggle.com/datasets/sudalairajkumar/novel-corona-virus-2019-dataset

Chen, Y. C., Lu, P. E., Chang, C. S., & Liu, T. H. (2020). A time-dependent SIR model for COVID-19 with undetectable infected persons. *Ieee transactions on network science and engineering*, *7*(4), 3279-3294. https://doi.org/10.1109/tnse.2020.3024723

Cooper, I., Mondal, A., & Antonopoulos, C. G. (2020). Dynamic tracking with model-based forecasting for the spread of the COVID-19 pandemic. *Chaos, Solitons & Fractals*, *139*, 110298. https://doi.org/10.1016/j.chaos.2020.110298

Djenina, N., Ouannas, A., Batiha, I. M., Grassi, G., Oussaeif, T. E., & Momani, S. (2022). A novel fractional-order discrete SIR model for predicting COVID-19 behavior. *Mathematics*, *10*(13), 2224. https://doi.org/10.3390/math10132224

Duan, Y. (2021, April). Simulations of the COVID-19 Epidemic in Nigeria Using SIR Model. In *Journal of Physics: Conference Series* (Vol. 1893, No. 1, p. 012016). IOP Publishing. https://doi.org/10.1088/1742-6596/1893/1/012016

Hanson, K. E., Caliendo, A. M., Arias, C. A., Englund, J. A., Lee, M. J., Loeb, M., ... & Mustafa, R. A. (2024). Infectious Diseases Society of America guidelines on the diagnosis of COVID-19 (June 2020). *Clinical infectious diseases*, *78*(7), e106-e132.

Lounis, M., & Bagal, D. K. (2020). Estimation of SIR model's parameters of COVID-19 in Algeria. *Bulletin of the National Research Centre*, *44*(1), 180. https://doi.org/10.1186/s42269-020-00434-5

Mbuvha, R., & Marwala, T. (2020). On data-driven management of the COVID-19 outbreak in South Africa. *medRxiv*, 2020-04. https://doi.org/10.1101/2020.04.07.20057133

Moein, S., Nickaeen, N., Roointan, A., Borhani, N., Heidary, Z., Javanmard, S. H., ... & Gheisari, Y. (2021). Inefficiency of SIR models in forecasting COVID-19 epidemic: a case study of Isfahan. *Scientific reports*, *11*(1), 4725. https://doi.org/10.1038/s41598-021-84055-6

Mojahid, H. Z., Zain, J. M., Basit, A., Yusoff, M., & Ali, M. (2024). A Review on Extensively Used Machine Learning Techniques for the Prediction of COVID-19. *Suranaree Journal of Science & Technology*, *31*(1). https://doi.org/10.55766/sujst-2024-01-e01334

Nesteruk, I. (2020). Simulations and predictions of COVID-19 pandemic with the use of SIR model. https://doi.org/10.20535/ibb.2020.4.2.204274

https://doi.org/10.24191/mij.v6i1.4625

Ni, G., Wang, Y., Gong, L., Ban, J., & Li, Z. (2022). Parameters sensitivity analysis of covid-19 based on the sceir prediction model. *COVID*, *2*(12), 1787-1805. https://doi.org/10.3390/covid2120129

Nicolle, L. E., Gupta, K., Bradley, S. F., Colgan, R., DeMuri, G. P., Drekonja, D., ... & Siemieniuk, R. (2019). Clinical practice guideline for the management of asymptomatic bacteriuria: 2019 update by the Infectious Diseases Society of America. *Clinical infectious diseases*, *68*(10), e83-e110. https://doi.org/10.1093/cid/ciy1121

Perakis, G., Singhvi, D., Skali Lami, O., & Thayaparan, L. (2023). COVID-19: A multiwave SIR-based model for learning waves. *Production and Operations Management*, *32*(5), 1471-1489. https://doi.org/10.1111/poms.13681

Putra, S., Mutamar, Z. K., & Zulkarnain, K. (2019). Estimation of parameters in the SIR epidemic model using particle swarm optimization. *Am. J. Math. Comput. Model*, *4*, 83-93. https://doi.org/10.11648/j.ajmcm.20190404.11

Rahimi, I., Gandomi, A. H., Asteris, P. G., & Chen, F. (2021). Analysis and prediction of COVID-19 using SIR, SEIQR, and machine learning models: Australia, Italy, and UK cases. *Information*, *12*(3), 109. https://doi.org/10.3390/info12030109

Saxena, R., Jadeja, M., & Bhateja, V. (2023). Propagation analysis of COVID-19: an SIR model-based investigation of the pandemic. *Arabian Journal for Science and Engineering*, *48*(8), 11103-11115. https://doi.org/10.1007/s13369-021-05904-0

Singh, R. A., Lal, R., & Kotti, R. R. (2022). Time-discrete SIR model for COVID-19 in Fiji. *Epidemiology & Infection*, *150*, e75. https://doi.org/10.1017/s0950268822000590

Vega, R., Flores, L., & Greiner, R. (2022). SIMLR: Machine Learning inside the SIR model for COVID-19 Forecasting. *Forecasting*, *4*(1), 72-94. https://doi.org/10.3390/forecast4010005

Venkatasen, M., Mathivanan, S. K., Jayagopal, P., Mani, P., Rajendran, S., Subramaniam, U., ... & Sorakaya Somanathan, M. (2020). Forecasting of the SARS-CoV-2 epidemic in India using SIR model, flatten curve and herd immunity. *Journal of ambient intelligence and humanized computing*, 1-9. https://doi.org/10.1007/s12652-020-02641-4

Worldometer. (2024, December 12). Population based on UN data for Malaysia country. *Worldometer*. https://www.worldometers.info/world-population/malaysia-population

Wu, J. (2023). The application of SIR model in COVID-19. *Theoretical and Natural Science*, *9*, 38-44. https://doi.org/10.54254/2753-8818/9/20240709

Yunus, A. A. M., Yunus, A. A. M., Ibrahim, M. S., & Ismail, S. (2021). Future of mathematical modelling: A review of COVID-19 infected cases using SIR model. *Baghdad Science Journal*, *18*(1 (Suppl.)), 0824-0824. https://doi.org/10.21123/bsj.2021

Zenian, S. (2022, August). The SIR model for COVID-19 in Malaysia. In *Journal of Physics: Conference Series* (Vol. 2314, No. 1, p. 012007). IOP Publishing. https://doi.org/10.1088/1742-6596/2314/1/012007